Computational Fluid Dynamics Analysis on the Upper Airways of Obstructive Sleep Apnea Using Patient – Specific Models

Y. Fan, L. K. Cheung, M. M. Chong, H. D. Chua, K. W. Chow, and C. H. Liu

Abstract—**Obstructive Sleep Apnea Syndrome (OSAS) is a common sleep disorder. It is characterized by repeated occlusion of upper airway and discontinuation of sleep. The breathing pauses and starts again with a loud snort. There may even be an abrupt interruption of sleep to maintain the patency of the airway. The pressure drop along the pharyngeal pathway should be a good indicator to show the severity of the pathological airways. Computational Fluid Dynamics (CFD) has become an important tool in investigating the internal flow dynamics of the respiratory system, especially for the upper airway. It provides a non–invasive environment for the analysis of the biological flow. Employing such technology, this study will provide insight for a male patient with severe OSAS. This patient also underwent surgical procedures to improve the size of the airway.**

The pre–operative and post–operative CT scans were reconstructed and converted to two patient–specific, three–dimensional models suitable for numerical simulations. The inhalation process was simulated using a constant volume flow rate, 0.3 liter per second (L s^{-1}), at the nostrils for both cases. An index, the 'resistance of the airway', was defined as the pressure drop per unit flow rate to estimate the tendency of airway collapse.

The pressure distribution from the velopharynx to hypopharynx was investigated. The pressure drops were 12.1 Pascal (Pa) and 7.3 Pascal before and after surgical treatment respectively. The resistance of airway changed from 40 Pa s L^{-1} to 24 Pa s L^{-1}, a 40% reduction.

The results showed that the pressure drop along the upper airway was reduced significantly after the surgical procedure. This decreased the collapsibility of the airway and consequently improved the sleep quality.

***Index Terms*—computational fluid dynamics, obstructive sleep apnea, patient specific model, upper airway**

Manuscript received March 28, 2011; revised April 10, 2011. Partial financial support has been provided by the Hong Kong Research Grants Council.

Y. Fan is with The Department of Mechanical Engineering, The University of Hong Kong, Pokfulam, Hong Kong (corresponding author to provide phone: (852) 2859 2641; fax: (852) 2858 5415; e-mail: siuyii@hku.hk).

L. K. Cheung, M. M. Chong and H. D. Chua are with The Discipline of Oral and Maxillofacial Surgery, Faculty of Dentistry, The University of Hong Kong, Pokfulam, Hong Kong (e-mail: lkcheung@hkucc.hku.hk; chongmei@hotmail.com; hdchua@gmail.com)

K. W. Chow and C. H. Liu are with the Mechanical Engineering Department, The University of Hong Kong, Pokfulam, Hong Kong (e-mail: kwchow@hku.hk; chliu@hkucc.hku.hk).

I. Introduction

OBSTRUCTIVE Sleep Apnea Syndrome (OSAS) is a common sleep breathing disorder (SBD). It is characterized by repeated occlusion of the upper airway and discontinuation of sleep (Fig. 1). This leads to low respiratory rate (hypopnea) or suspension of breathing (apnea). Once the upper airway collapses (mostly occurs at the retroplatal and retroglossal regions), the respiratory effort increases. The breathing pauses and starts again with a loud snort. There may even be an abrupt interruption of sleep to maintain the patency of the airway [1]–[6].

There is a serious and rapid increase in the incidence of the sleep disorder and related diseases. The prevalence of OSAS in Hong Kong is similar to that in the United States (4% in men, 2% in women) [5]–[6]. However, most of the people underestimated the consequences of the obstructive sleep apnea syndrome, 82–98% adults in the United States are underdiagnosed [3] & [7].

A. Risk Factors

The major structures of the upper airway are the soft tissues and the skeleton. The dysfunction or deformities of them are the main constituents for the pathogenesis of OSAS. Obesity and craniofacial factors are two major contributed elements for OSAS. The pharyngeal wall is elastic and expansible at which is free from the support of the cartilages. In the obese patients, the bulky pharyngeal tissues narrow the air pathway. The Asian groups are relatively less likely to be overweight than the Caucasian counterparts. The craniofacial parts then become a bigger contributor to the development of OSAS in this predominantly Chinese population [1].

B. Symptoms and Consequences

Due to the morphological differences in the upper airways, most of the patients share some general signs and symptoms, such as loud snoring, excessive daytime sleepiness and morning headaches. The poor quality of sleep seriously affects the daily life and health conditions of the patients. The daytime fatigue and headache have a negative impact on the efficiency at the workplace. It has also been reported that OSAS patients are more likely to have motor vehicle accidents [3]. Earlier studies showed that the OSAS patients may have serious cardiovascular, pulmonary and neurologic

problems [2]. This disorder also increases the risk of stroke and death [2]–[4].

C. Treatments

OSAS is a treatable form of sleep breathing disorder. The goals of treatments are to keep the airway open and to prevent the pause of breathing during sleep. Continuous positive airway pressure (CPAP) is the first–line, non–invasive treatment for most of the patients [3]–[4]. The PAP devices produce a pressurized airflow to the patient via a facial mask during sleep.

For severe cases, invasive surgical procedures may be carried out. In our work, mandibular distraction was performed on a severe OSAS patient. The distraction is a method to increase the length of the lower jaw bone as well as the size of the pharyngeal airway.

D. Literature Review

Employing the computational fluid dynamics (CFD) technique on the study of obstructive sleep apnea syndrome is a very new aspect in biomedical engineering. In 2006, Xu reported a CFD investigation of the airflow in the upper airways of six subjects [8]. After his work, several authors discussed the effect of the inspiration rate on the aerodynamics of the upper airway [9]–[10]. Another group of researchers described the effectiveness of the mandibular advancing surgery with maxillomandibular advancement [11]–[14]. Although some of them published a large scale study of the OSAS patients using mandibular repositioning appliances, there is still a research gap for the patients who have undergone the mandibular distraction.

Computational fluid dynamics proves to be a convenient and reliable tool for simulating the internal flow dynamics of the respiratory system [8]–[16]. CFD gives a prediction on the pressure distribution, flow velocities, and other physical properties. We built patient–specific, three–dimensional models in order to analyze the flow dynamics inside the pharynx without complicated *in vivo* experiments.

The main objective of this study is to analyze the morphological changes, the pressure distribution and the airway resistance of a severe OSAS patient, before and after the surgical procedure, by CFD.

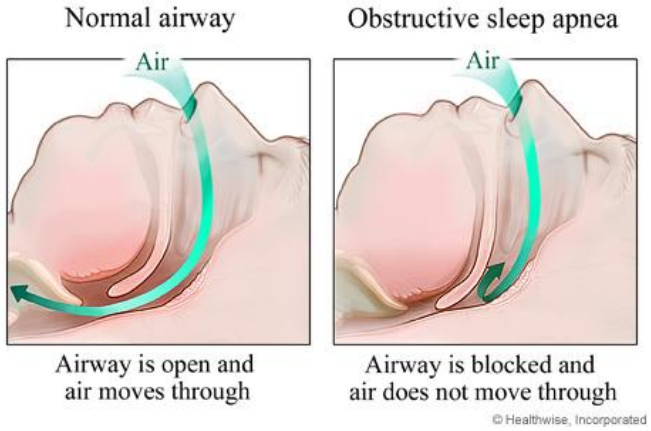

Fig. 1 The diagram shows the difference on the airflow between a normal airway and an obstructed airway.

II. Methods

Computational fluid dynamics is a widely used tool for the prediction of the biological flow in the respiratory system. Using similar methodology in the previous literatures, the three–dimensional patient–specific models were reconstructed and will be applied in the computation.

High–resolution cone–beam Computerized Tomography (CBCT) images were obtained for the construction of the patient–specific models. The mesh and mathematical models were treated by sophisticated commercial software. The flow patterns and streamlines were simulated by CFD. Subsequently, the pressure distribution could then be analyzed.

A. Patient Characteristics

The patient under consideration is a 45–year–old Chinese man. The body mass index (BMI) is 21 kg m^{-2} which is classified as 'Normal'. He was diagnosed with severe Obstructive Sleep Apnea Syndrome, as well as severe mandibular hypoplasia due to condylar resorption, which means an unusually small size of the lower jaw. In order to improve the quality of sleep, the patient underwent the surgical intervention to lengthen the mandible and to expand the pharyngeal pathway. The procedure included the intraoral distraction of the mandible and bilateral condylar shaving. The pre– and post– operative CBCT data files were used for 3D reconstruction. The post–operative data was obtained on the sixth year after the surgical treatment.

B. Patient-Specific Modeling

There were totally 323 two–dimensional images in each case for the 3D model reconstruction of the mathematical models. Each image was separated by a 0.3 mm distance. The CT DICOM (Digital Imaging and Communications in Medicine) images were imported into commercial software (Mimics 13.0, Materialise, Belgium). The models included the nostrils, the nasal cavity, the nasopharynx, velopharynx, and oropharynx and ended below the epiglottis (Fig. 2).

The reconstruction of the upper airway was based on the Hounsfield Units (HU) value, a measure of the electron density of the tissue, in the CT images. The HU value of air in the CT images ranged from -1000 to -500. The 3D models were then smoothed and meshed in 3–matic (Materialise, Belgium), and finally exported for further analysis (Fig. 3). Volume meshing was generated with reference to the surface mesh using the package TGrid 5.0.6 (ANSYS, Canonsburg, USA). High quality, unstructured grids were created. There were totally 4.4×10^5 and 1.5×10^6 cells in the pre–operative and post–operative models respectively. Mesh independent test was taken.

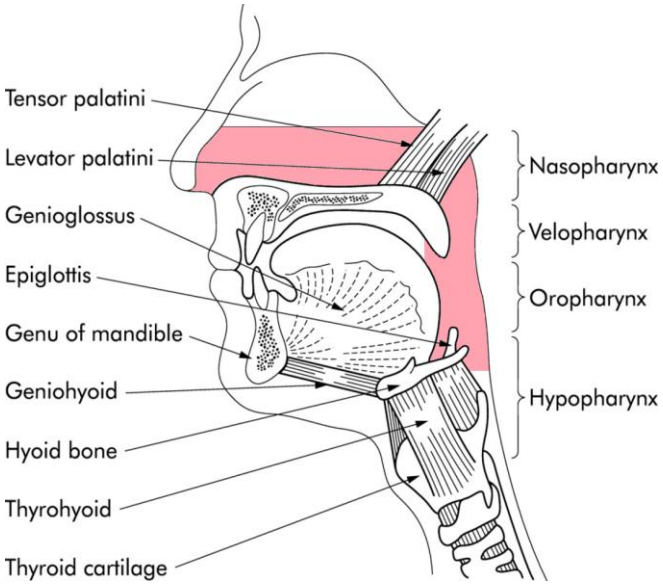

Fig.2 Anatomy of the upper airway. The part of interest is highlighted.

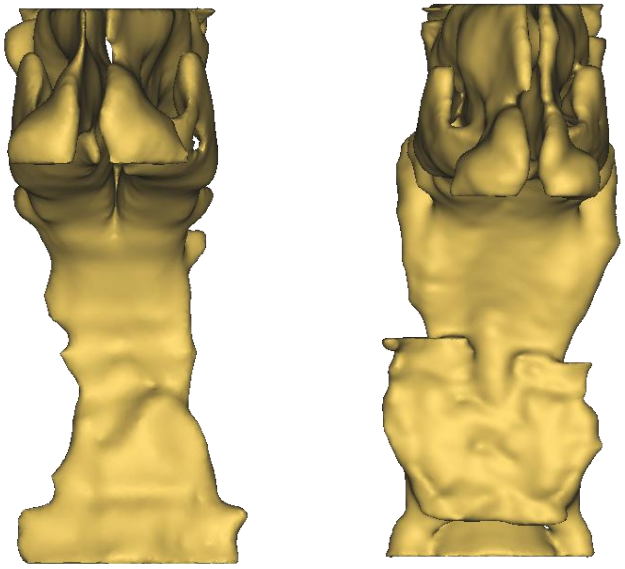

(a) (b)

Fig.3 The front view of the three–dimensional physiological models, (a) before surgical treatment, and (b) after surgical procedure.

C. Boundary Conditions

FLUENT 6.3.26 (ANSYS, Canonsburg, USA) was employed for the steady airflow simulation. The nostrils were defined as the location for velocity inlets, while the outlet boundary was situated just below the epiglottis. In previous literatures, the inspiration rates used were in a large range from 179 mL s^{-1} to 500 mL s^{-1} [10] & [13]. The velocities prescribed at the inlets were varied to match with the constant volume flow rate 300 mL s^{-1}. The pressure was set to be zero Pascal (Pa) at the outlet to mimic the normal breathing during inhalation. No–slip boundary conditions were applied on the walls of the airway. The compliance of the airway was neglected.

The governing equations of fluid motion were the usual continuity equation (conservation of mass), and the Navier–Stokes (NS) equations (rate of change of momentum). In tensor notations (repeated indices implying summation), the continuity equation is

$$\frac{\partial u_i}{\partial x_i} = 0 , \qquad (1)$$

and the three dimensional NS equations are

$$\frac{\partial u_i}{\partial t} + u_j \frac{\partial u_i}{\partial x_j} = -\frac{1}{\rho}\frac{\partial p}{\partial x_i} + \frac{1}{\rho}\frac{\partial \tau_{ij}}{\partial x_j} . \qquad (2)$$

Where ρ = fluid density; u_i (i=1,2,3) = components of velocity vector; τ_{ij} = normal and shear stresses; p = pressure.

In terms of material properties, the density of air was taken as 1.225 kg m^{-3}, and the viscosity was assumed to be 1.789 x 10^{-5} kg m^{-1} s^{-1}. The Reynolds numbers at the inlets were around 1836 and 1614 for the pre–operative and post–operative models respectively. The Reynolds number still fell in the laminar regime. However, the cross–sectional area along the nasal airway was very small and the Reynolds number may fall into the turbulent region. The flow in the upper airway was assumed to be incompressible and turbulent. The low Reynolds number $k - \varepsilon$ turbulent model was applied for the simulations.

D. Resistance of Upper Airway

The muscles of the pharyngeal airway relax during sleep. The local negative intraluminal pressure would result in collapse and obstruction of the airway. The focus of this study is on the pressure distribution as well as the pressure difference along the pharynx. We divided the pharynx, from the level of hard palate to the plane of outlet, into twenty–one transversal planes to investigate the change in pressure and the change in the size of the cross–sectional area. The computations would give a pressure difference (ΔP) for a flow rate (Q) inside the airway. The resistance of the airway (R) could then be determined using equation (3), using a principle similar to Ohm's law (resistance equals voltage divided by the current).

$$R = \frac{\Delta P}{Q} \qquad (3)$$

III. Results

Two cases, the pre–operation and post–operation configurations, of a severe OSAS patient were analyzed in this study. The main focus of the analysis was the region within the velopharynx, from the level of hard palate (A_{first}) to the level of epiglottis (Outlet) (Fig. 4). Twenty–one planes were defined along this portion in order to investigate the pressure variation at different locations. The first plane, A_{first}, was at the level of hard palate and the last plane was at the outlet, while the planes in between are equally spaced (Fig. 4).

A. Morphology of Airway

From the reconstructed physiological models, we can easily see the differences in the sizes of the airways. Three–dimensional expansion was noticed in the pharynx which may give a better environment for breathing (Figs. 3 & 4). This expansion can be quantified by calculating the percentage of the stenosis of the pharynx. The plane with minimum area, A_{min}, was compared with the first plane, A_{first} (Fig. 4). Figure 5 showed the variation of the cross–sectional area along the pharynx before and after the surgical procedure. The graph clearly showed that the dimensions of the airway were expanded successfully by the intra–oral mandibular distraction. The dimensions of the minimum areas were increased from 0.6 cm^2 to 1.7 cm^2. When comparing these values with the sizes at the level of hard palate, A_{first}, the percentage of stenosis can be estimated by:

$$Percentage \quad of \quad stenosis \quad = \quad \left(1 - \frac{A_{min}}{A_{first}}\right) \times 100 \ \%$$

The percentage of stenosis improved from 80.5% to 49.0% after the surgical treatment (Table I).

B. Airway Resistance

During inhalation, the atmospheric pressure was higher than the pressure in the lungs. The pressure difference drove the inflow of air. Figure 6(a) showed the vector plots of velocity magnitude at the mid–sagittal plane of the pre–operative pharynx. The red color at the narrowest region represented a very high speed flow at 5.7 m s^{-1}. While the vector plot of the post–operative model only showed a gradual change in the velocity (Fig. 6).

According to the Bernoulli's Principle, for an inviscid fluid, an increase in the speed of the fluid occurs simultaneously with a decrease in pressure. The lowest pressure was illustrated at the narrowest part of the airway (Figs. 7 & 8). For an OSAS patient, a greater pressure was required for driving the air into the restricted airway. The local pressure reduced to a negative value and the minimum pressure was –6 Pascal (Pa) (Fig. 9).

The pressure difference between the first and the twenty–first planes was 12.1 Pa. After the mandibular distraction, no negative pressure was recorded along the pharynx and only a gradual decrease in the pressure was resulted which was 7.3 Pa. With a constant volume flow rate, 0.3 L s^{-1}, the resistances were 40.2 Pa s L^{-1} and 24.3 Pa s L^{-1} before and after treatment respectively (Table I).

TABLE I
COMPARISON BETWEEN PRE-OPERATION AND POST-OPERATION

	A_{first} (cm^2)	A_{min} (cm^2)	Percentage of Stenosis	Resistance (Pa s L^{-1})
Pre–operation	3.3	0.6	80.5%	40.2
Post–operation	3.3	1.7	49.0%	24.3

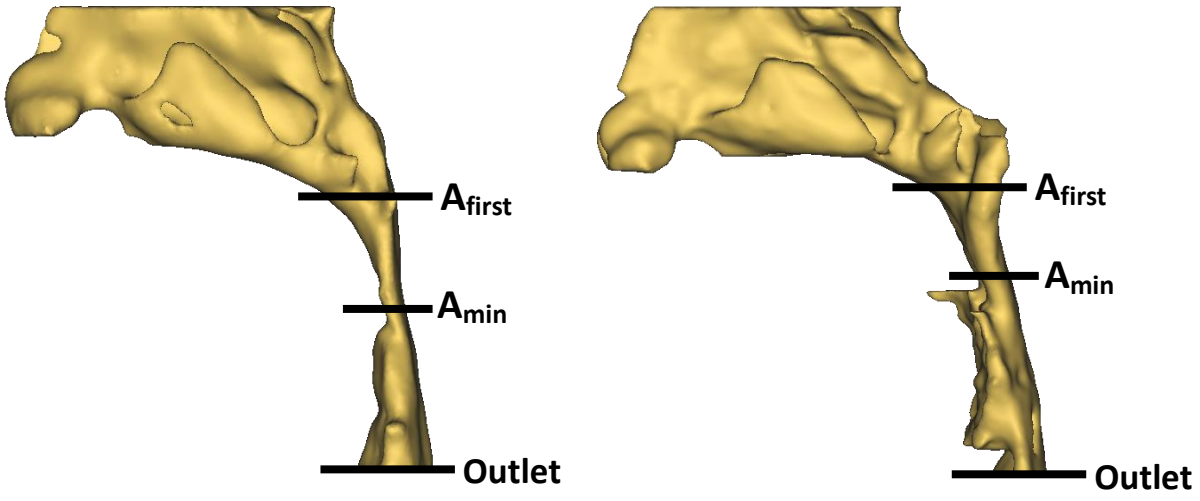

(a) (b)

Fig. 4 The left view of the three–dimensional physiological models, (a) before surgical treatment, and (b) after surgical procedure. The definitions of A_{first}, A_{min}, and outlet.

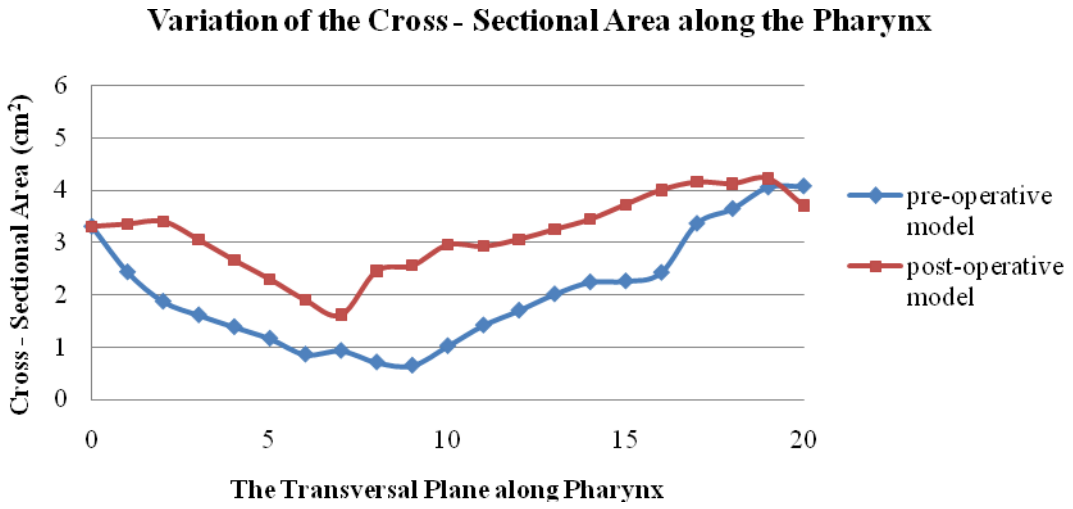

Fig. 5 The graph showing the variation of the cross–sectional area along the pharynx.

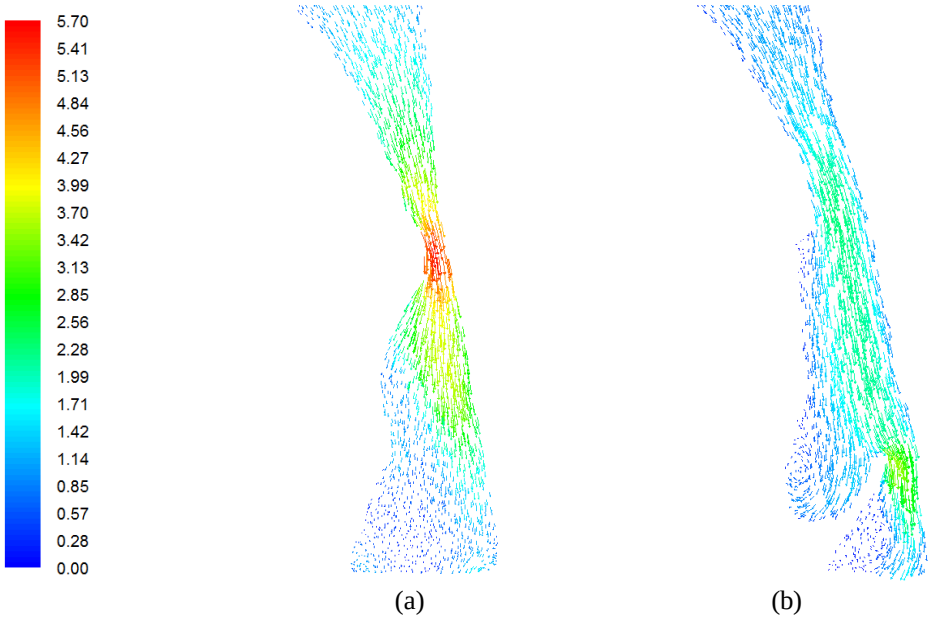

Fig. 6 Velocity vectors at the mid – sagittal planes (a) before operation; (b) after mandibular distraction of an OSA patient. The color scale representing the velocity magnitude.

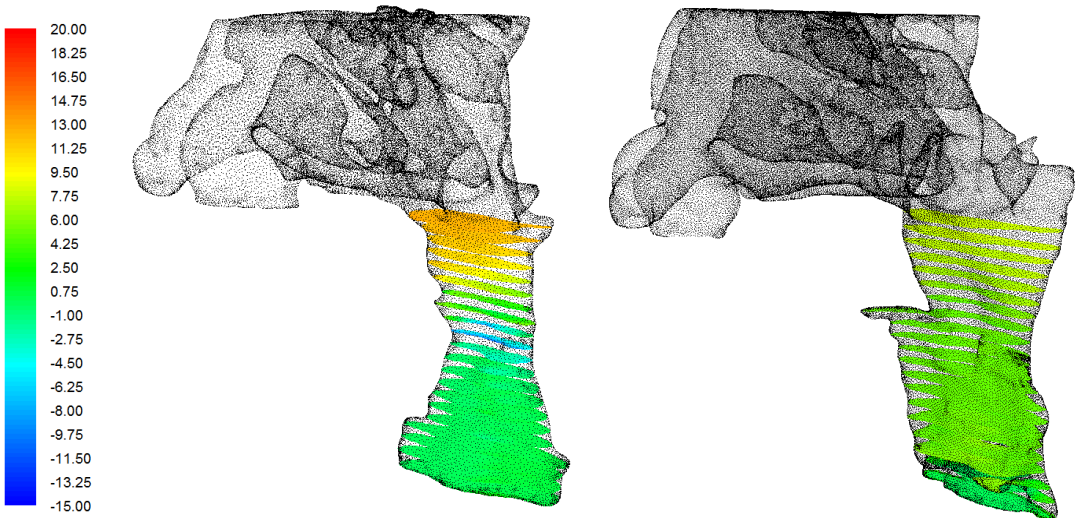

Fig. 7 Pressure distribution at twenty–one transversal planes along the pharynx (a) before operation; (b) after mandibular distraction, of an OSA patient.

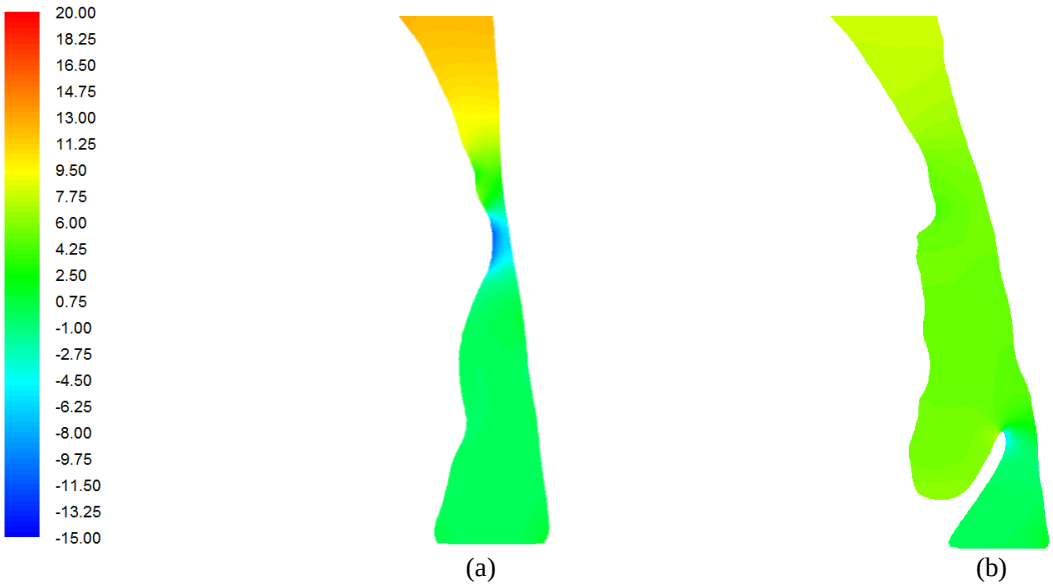

Fig. 8 Contours of pressure at the mid–sagittal plane along the pharynx (a) before operation; (b) after mandibular distraction, of an OSA patient.

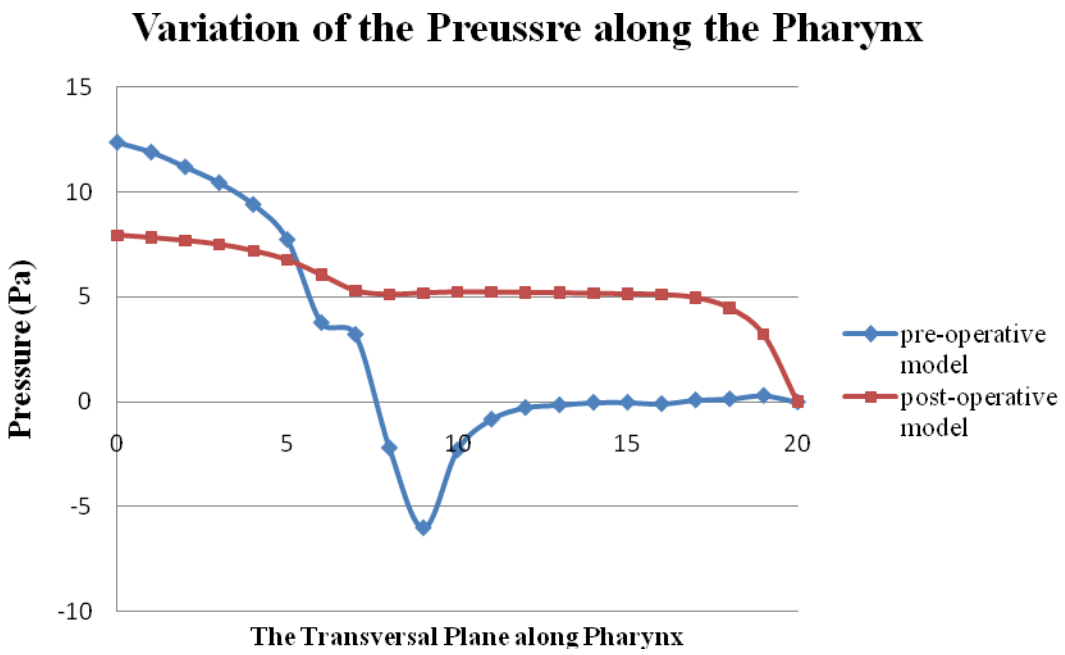

Fig. 9 The graph showing the variation of pressure along the pharynx for pre – operative model and post – operative model.

IV. Discussion

Two main parameters were studied to investigate the effect of mandibular distraction. The minimum cross–sectional area in the upper airway increased threefold, from 0.6 cm^2 to 1.7 cm^2. The triple enlargement of the area caused a sharp drop in the percentage of stenosis. This widened airway highly reduced the chance of collapse and blockage during inspiration. The widened airway gave a better flow environment which has been illustrated in the pressure distribution. The minimum pressure, –6 Pa, was recorded at the oropharynx section before surgical treatment. The negative intraluminal pressure promoted the development of airway obstruction. The airway resistance of the airway also dropped significantly, from 40.2 Pa s L^{-1} to 24.3 Pa s L^{-1}. This implied that the air could be breathed in more easily. The 40% reduction in the resistance reduced the collapsibility of the pharyngeal airway. The quality of sleep would therefore be improved.

V. Conclusion

The pressure distribution and the resistance in the upper airway of the obstructive sleep apnea patient were studied using computational fluid dynamics. In order to mimic a physiological environment, three–dimensional patient–specific models were created using CT images of a severe OSAS patient.

The computational results showed a significant improvement in the breathing environment during inspiration after the distraction of the mandible. The 40% decrease in the airway resistance highly reduced the collapsibility of the pharyngeal airway.

References

[1] R. W. W. Lee, S. Vasudavan, D. S. Hui, T. Prvan, P. Petocz, M. Ali Darendeliler, P. A. Cistulli, "Differences in craniofacial structures and obesity in Caucasian and Chinese patients with obstructive sleep apnea," *Sleep*, vol. 33, no. 8, pp.1075–1080, Feb. 2010.

[2] H. K. Yaggi, J. Concato, W. N. Kernan, J. H. Lichtman, L. M. Brass, v. Mohsenin, "Obstructive sleep apnea as a risk factor for stroke and death," *N. Engl. J. Med.*, vol. 353, pp. 2034–2041, Nov. 2005.

[3] T. Young, P. E. Peppard, D. J. Gottlleb, "Epidemiology of obstructive sleep apnea: a population health perspective," *Am. J. Respir. Crit. Care Med.*, vol. 165, pp. 1217–1239, May. 2002.

[4] T. Young, P. E. Peppard, J. Skatrud. "Risk factors for obstructive sleep apnea in adults," *J. Am. Med. Assoc.*, vol. 291, no. 16, pp. 2013–2016, Apr. 2004.

[5] M. S. M. Ip, B. Lam, I. J. Lauder, K. W. T. Tsang, K. F. Chung, Y. W. Mok, W. K. Lam, "A community study of sleep-disordered breathing in middle-aged Chinese men in Hong Kong," *Chest*, vol. 119, pp. 62–69, Jan. 2001.

[6] M. S. M. Ip, B. Lam, L. C. H. Tang, I. J. Lauder, T. Y. Ip, W. K. Lam, "A community study of sleep-disordered breathing in middle-aged Chinese women in Hong Kong prevalence and gender differences," *Chest*, vol. 125, no. 1, pp. 127–134, Jan. 2004.

[7] J. E. Remmers, W. J. deGroot, E. K. Sauerland and A. M. Anch, "Pathogenesis of upper airway occlusion during sleep," *Journal of Applied Physiology*, vol. 44, pp. 931-938, 1978.

[8] C. Xu, S. H. Sin, J. M. McDonough, J. K. Udupa, A. Guez, R. Arens and D. M. Wootton, "Computational fluid dynamics modeling of the upper airway of children with obstructive sleep apnea syndrome in steady flow," *Journal of Biomechanics*, vol. 39, pp. 2043-2054, 2006.

[9] M. Mihaescu, S. Murugappan, E. Gutmark, L. F. Donnelly, S. Khosla, M. Kalra, "Computational fluid dynamics analysis of upper airway reconstructed from magnetic resonance imaging data," *Ann. Otol. Rhinol. Laryngol.*, vol. 117, no. 4, pp. 303–309, Apr. 2008.

[10] S. J. Sung, S. J. Jeong, Y. S. Yu, C. J. Hwang, E. K. Pae, "Customized three-dimensional computational fluid dynamics simulation of the upper airway of obstructive sleep apnea," *Angl. Orthod.*, vol. 76, no. 5, pp. 791–799, Sept. 2006.

[11] J. W. DeBacker, O. M. Vanderveken, W. G. Vos, A. Devolder, S. L. Verhulst, J. A. Verbraecken, P. M. Parizel, M. J. Braem, P. H. Van DeHeyning and W. A. De Backer, "Functional imaging using computational fluid dynamics to predict treatment success of mandibular advancement devices in sleep-disordered breathing," *Journal of Biomechanics*, vol. 40, pp. 3708-3714, 2007.

[12] C. Van Holsbeke, J. DeBacker, W. Vos, P. Verdonck, P. Van Ransbeeck, T. Claessens, M. Braem, O. Vanderveken and W. DeBacker, "Anatomical and functional changes in the upper airways of sleep apnea patients due to mandibular repositioning: a large scale study," *Journal of Biomechanics*, vol. 44, p. 442-449, 2011.

[13] C. C. Yu, H. D. Hsiao, L. C. Lee, C. M. Yao, N. H. Chen, C. J. Wang, Y. R. Chen, "Computational fluid dynamics study on obstructive sleep apnea syndrome treated with maxillomandibular advancement," *Journal of Craniofacial Surgery*, vol. 20, no. 2, pp. 426–430, Mar. 2009.

[14] J. Huynh, K. B. Kim and M. McQuilling, "Pharyngeal airflow analysis in obstructive sleep apnea patients pre- and post- maxillomandibular advancement surgery," *Journal of Fluids Engineering*, vol. 131, 091101, 2009.

[15] J. W. De Backer, W. G. Vos, C. D. Gorlé, P. Germonpré, B. Partoens, F. L. Wuyts, P. M. Parizel, W. De Backer, "Flow analyses in the lower airways: patient-specific model and boundary conditions," *Med. Eng. & Phys.*, vol. 30, no. 7, pp. 872–879, Sept. 2008.

[16] Y. Fan, L. K. Cheung, M. M. Chong, K. W. Chow, C. H. Liu, "Computational study on obstructive sleep apnea syndrome using patient–specific Models," *Lecture Notes in Engineering and Computer Science: Proceedings of The World Congress on Engineering 2011*, WCE 2011, 6-8 July, 2011, London, U.K., pp. 2632–2635.